Experimental Animals
Exp. Anim. 71(3), 288–304, 2022

Original

The C-type lectin receptor Clec1A plays an important role in the development of experimental autoimmune encephalomyelitis by enhancing antigen presenting ability of dendritic cells and inducing inflammatory cytokine IL-17

Yulia MAKUSHEVA[1)], Soo-Hyun CHUNG[1)], Aoi AKITSU[1,2)], Natsumi MAEDA[1,3)], Takumi MARUHASHI[1,4)], Xiao-Qi YE[1,5)], Tomonori KAIFU[1,6)], Shinobu SAIJO[7)], Haiyang SUN[1)], Wei HAN[1)], Ce TANG[1,5)] and Yoichiro IWAKURA[1)]

[1)]*Center for Animal Disease Models, Research Institute for Biomedical Sciences, Tokyo University of Science, 2669 Yamazaki, Noda, Chiba 278-0022, Japan*
[2)]*Present address: Laboratory of Immunobiology, Department of Medical Oncology, Dana-Farber Cancer Institute, Harvard Medical School, 450 Brookline Avenue, Boston, MA 02215, U.S.A.*
[3)]*Present address: Laboratory for Prediction of Cell Systems Dynamics, RIKEN Center for Biosystems Dynamics Research, 6-2-3 Furuedai, Suita, Osaka 565-0874, Japan*
[4)]*Present address: Laboratory of Molecular Immunology, Institute for Quantitative Biosciences, The University of Tokyo, 1-1-1 Yayoi, Bunkyo-ku, Tokyo 113-0032, Japan*
[5)]*Institute of Precision Medicine, The First Affiliated Hospital, Sun Yat-sen University, 58 Zhongshaner Road, Yuexiu District, Guangzhou, Guangdong Province 510080, P.R. China*
[6)]*Present address: Division of Immunology Faculty of Medicine, Tohoku Medical and Pharmaceutical University, 1-15-1 Fukumuro, Miyagino-ku, Sendai, Miyagi 983-8536, Japan*
[7)]*Medical Mycology Research Center, Chiba University, 1-8-1 Inohana, Chuo-ku, Chiba 260-8673, Japan*

Abstract: Clec1A, a member of C-type lectin receptor family, has a carbohydrate recognition domain in its extracellular region, but no known signaling motif in the cytoplasmic domain. *Clec1a* is highly expressed in endothelial cells and weakly in dendritic cells. Although this molecule was reported to play an important role in the host defense against *Aspergillus fumigatus* by recognizing 1,8-dihydroxynaphthalene-melanin on the fungal surface, the roles of this molecule in un-infected animals remain to be elucidated. In this study, we found that *Clec1a*$^{-/-}$ mice develop milder symptoms upon induction of experimental autoimmune encephalomyelitis (EAE), an animal model for multiple sclerosis. The maximum disease score was significantly lower, and demyelination and inflammation of the spinal cord were much milder in *Clec1a*$^{-/-}$ mice compared to wild-type mice. No abnormality was detected in the immune cell composition in the draining lymph nodes and spleen on day 10 and 16 after EAE induction. Recall memory T cell proliferation after restimulation with myelin oligodendrocyte glycoprotein peptide ($MOG_{35–55}$) *in vitro* was decreased in *Clec1a*$^{-/-}$ mice, and antigen presenting ability of *Clec1a*$^{-/-}$ dendritic cells was impaired. Interestingly, RNA-Seq and RT-qPCR analyses clearly showed that the expression of inflammatory cytokines including *Il17a*, *Il6* and *Il1b* was greatly decreased in *Clec1a*$^{-/-}$ mice after induction of EAE, suggesting that this reduced cytokine production is responsible for the amelioration of EAE in *Clec1a*$^{-/-}$ mice. These observations suggest a novel function of Clec1A in the immune system.
Key words: Clec1a, C-type lectin receptor, experimental autoimmune encephalomyelitis, IL-17

(Received 2 December 2021 / Accepted 3 January 2022 / Published online in J-STAGE 8 February 2022)
Corresponding author: Y. Iwakura. email: iwakura@rs.tus.ac.jp
Supplementary Figures: refer to J-STAGE: https://www.jstage.jst.go.jp/browse/expanim

This is an open-access article distributed under the terms of the Creative Commons Attribution Non-Commercial No Derivatives (by-nc-nd) License <http://creativecommons.org/licenses/by-nc-nd/4.0/>.
©2022 Japanese Association for Laboratory Animal Science

Introduction

Multiple sclerosis is an autoimmune disease that affects the central nervous system (CNS) and causes various symptoms including fatigue, vision dysfunction, muscle weakness, and pain [1, 2]. Although the etiology and pathogenesis are not known completely, the main mechanisms of the disease are suggested to be autoimmune in nature and involve breakdown of blood-brain barrier and inflammatory cell infiltration into the central nervous system, resulting in demyelination and oligodendrocyte cell death [3–5]. Experimental autoimmune encephalomyelitis (EAE) is a commonly used mouse model of multiple sclerosis, and in this model, myelin oligodendrocyte-specific immune responses are induced by injecting myelin oligodendrocyte glycoprotein peptide ($MOG_{35–55}$) [4, 6]. In this model, an inflammatory cytokine IL-17A, which is produced by Th17 cells as well as γδ T cells [7, 8], plays a central role for the development of disease by activating other immune cells and recruiting neutrophils to the CNS [9–11]. Although this model has some limitations as not all traits are similar to human disease, this is a valuable instrument in the analysis of multiple sclerosis *in vivo* [4, 12].

C-type lectin receptor (CLR) is an innate immune receptor that is mainly involved in the host defense against pathogens. CLRs recognize carbohydrate molecules on the pathogen surface by a carbohydrate recognition domain (CRD) of the molecule in a calcium-dependent manner [13–16], and transduce positive or negative signaling through the immunoreceptor tyrosine-based activating motif (ITAM) or immunoreceptor tyrosine-based inhibitory motif (ITIM) in the cytoplasmic domain, respectively. CLRs are particularly known to be crucial for the host defense against fungi and extracellularly growing bacteria [17–21]. CLRs can also recognize a number of other ligands than carbohydrate molecules and are involved in various processes including dead cell sensing and removal [22–24], cancer cell recognition [25, 26], and inflammatory diseases [27–30]. Furthermore, several CLRs were shown to mediate the development of EAE [31, 32].

Clec1A is one of CLRs that is also called MelLec or Clec1. Although this receptor was first described more than twenty years ago, it remains poorly characterized [33, 34]. Structural analysis of Clec1A shows that it possesses a conventional carbohydrate recognition domain and a transmembrane domain. However, no sequence similar to ITAM or ITIM is detected, suggesting that Clec1A may have other mechanisms for the signal transduction [34]. This receptor also lacks sequence important for classic Ca^{2+}-dependent binding, thus it may suggest existence of alternative ligands other than carbohydrates [33]. Quantitative RT-PCR examination showed high levels of *Clec1a* mRNA expression in lungs, lymph nodes (LNs), spleen, and aorta of rats [35]. Flow cytometric analysis demonstrated that in mice this protein is highly expressed on CD45-negative CD31-positive endothelial cells of lungs, liver, heart, kidney, and small intestine while no expression was detected on CD45-positive leukocytes [36]. On the other hand, Robles *et al.* reported that human Clec1A is expressed on blood DCs, monocyte-derived DCs and monocytes, and is responsible for dampening the activation of these cells and Th1 and Th17 responses [37]. Screening of Clec1A ligands by analyzing Clec1A-Fc binding to various fungal species by flow cytometry revealed that 1,8-dihydroxynaphthalene-melanin in *Aspergillus fumigatus* (*A. fumigatus*) is one of the ligands [36]. Upon infection with *A. fumigatus*, Clec1A plays a key role in the antifungal immunity by inducing CXCL1 and CCL2 and recruiting neutrophils through recognition of the fungal ligand. Furthermore, a single nucleotide polymorphism in humans suggests that Clec1A also plays an important role for the protection against fungi in humans [36].

Many CLRs are involved not only in the host defense against pathogens, but also in the regulation of the immune system and the development of autoimmunity and tumors. For example, Mincle is important for the defense against fungi and mycobacteria, and also suppresses anttumor immunity by promoting myeloid-derived-suppressor-cell-mediated immune suppression via recognition of damaged cell-derived SAP-130 [38]. Dectin-1 is important not only in the defense against fungal infection but also in eradication of tumors and regulation of colitis [27, 39, 40]. Furthermore, we showed that many CLRs are involved in the regulation of the immune system and development of autoimmune and allergic diseases [27, 29, 32, 41–43]. Since the structure of Clec1A is quite unique and distinct from other CLR family members, we are very much interested in the roles of this molecule in other immune functions than anti-fungal immunity. Because Clec1A can induce CXCL1 and CCL2 and recruit neutrophils, it seemed likely that Clec1A is also involved in inflammatory process. Thus, we examined the effects of Clec1A-deficiency on the development of EAE. We found that the development of EAE was significantly suppressed in *Clec1a*$^{-/-}$ mice, suggesting a novel function for Clec1A in the regulation of an inflammatory CNS disease.

Materials and Methods

Mice

C57BL/6J mice (designated as wild-type, WT, mice) were obtained from CLEA Japan (Tokyo, Japan) and were housed in the same facility as *Clec1a*$^{-/-}$ mice. Eight to thirteen-week-old mice of the same sex were used for the experiments. 2D2 TCR transgenic (2D2 Tg) mice were purchased from the Jackson Laboratory. All mice were kept under specific pathogen-free conditions with γ-ray sterilized normal diet (F1, Funabashi Farm, Chiba, Japan), acidified (0.002 N HCl, pH 2.5) tap water, and autoclaved wooden chip bed in environmentally controlled clean rooms at the Center for Animal Disease Models, Research Institute for Biomedical Sciences, Tokyo University of Science. The experiments were carried out according to the institutional ethical guidelines for animal experiments and the safety guidelines for gene manipulation experiments, after approval by the institutional committees.

Generation of *Clec1a*$^{-/-}$ mice

Clec1a$^{-/-}$ mice were generated using homologous recombination techniques. Briefly, DNA fragments for the 5' and 3' homologous arms (1.4 and 8.0 kbp, respectively) were amplified by PCR from the C57BL/6J mouse BAC library containing *Clec1a* gene (RP23-394L7, Advanced GenoTechs Co., Tsukuba, Japan). The targeting vector was constructed by replacing the genomic region containing the initiation codon in the exon 1 of the *Clec1a* gene with the DNA fragment containing the *EGFP* gene and the neomycin resistance gene under the phosphoglycerate kinase 1 promoter (Neo^{r}) which was flanked by lox P sequences (Supplementary Fig. 1). A diphtheria toxin A fragment under the control of MC1 promoter (DT-A) was ligated at the 3' end of the targeting vector for negative selection. The targeting vector was linearized by *Sac*II digestion, and electroporated into C57BL/6N mouse ES cells (EGR-101), and G418 resistant colonies were selected. Homologous recombinants were screened by Southern blot hybridization analysis with the 3' and Neo^{r} probes. A clone of targeted ES cells was used for generation of chimeric mice by an aggregation method [39]. To generate heterozygous offspring, male chimeric mice were mated with C57BL/6J female mice. Genotypes were determined by PCR with the following primer-sets; Common forward: 5'-GTGAATAATGCGTTGCTCTCTGCC-3', WT reverse: 5'-GATGTGCTCAGATTGCTCGAGAGG-3', and Mutant (EGFP) reverse: 5'-CTGAACTTGTGGCCGTTTACGTCG-3'. The lack of *Clec1a* transcript was confirmed by quantitative real-time PCR. *Clec1a*$^{-/-}$ mice were obtained by intercrossing *Clec1a*$^{+/-}$ mice, then heterozygous embryos obtained by backcrossing to a C57BL/6J mouse were frozen at F7 generation. After recovery, *Clec1a*$^{-/-}$ mice were obtained by intercrossing these *Clec1a*$^{+/-}$mice, and maintained as a homozygous deficient state for 8~14 generations, and used for the experiments.

EAE model

EAE was induced according to the protocol of active immunization [6]. Eight to twelve-week-old male and female mice were subcutaneously (s.c.) immunized with 100 μl of emulsion containing 100 μg myelin oligodendrocyte glycoprotein (MOG) peptide (MEVGWYRSPFSRVVHLYRNGK: $MOG_{35–55}$, Scrum Inc., Tokyo, Japan) in Incomplete Freund Adjuvant (Thermo Scientific, Waltham, MA, USA) supplemented with 500 μg of heat-killed (hk)-*Mycobacterium (M.) tuberculosis* H37RA (BD difco, Sparks, MD, USA) (CFA) on day 0. On the same day and day 2, mice were injected intraperitoneally (i.p.) with 200 ng of pertussis toxin (PTX) (List Biological Laboratories, Campbell, CA, USA). MOG/CFA injection was repeated on day 7. Mice were followed up until day 28 and disease score was assessed daily as follows: 0 − normal; 0.5 − partially paralyzed tail; 1 − complete tail paralysis; 2 − weakness in hind limbs; 2.5 − one hind limb paralyzed; 3 − two hind limbs paralyzed; 3.5 − weakness in fore limbs; 4 − paralysis of one fore limb; 4.5 − paralysis of both fore limbs; 5 − moribund state.

Histological staining

Samples of the spinal cord were collected from WT and *Clec1a*$^{-/-}$ mice at day 28 after induction of EAE. Mice were euthanized, spinal cords were excised and fixed in 10% neutral-buffered formalin. L1-L5 region was dehydrated in ethanol gradients, paraffin embedded, and cut to 10 μm sections by GenoStaff Co., Japan. After rehydration, the specimens were stained with hematoxylin and eosin.

The same paraffin-embedded samples of the spinal cord were cut into 10 μm, and after dehydration, stained by Luxol Fast Blue and counterstained with Cresyl Violet. Images were observed under a Keyence BZ-9000 microscope (Osaka, Japan) and analyzed by ImageJ software (National Institutes of Health, Bethesda, MD, USA).

RNA-Seq analysis

Inguinal draining LNs (dLNs) from WT and *Clec1a*$^{-/-}$ mice (n=5 in each group) were collected in a steady-state and at day 10 and 16 after EAE induction. Total RNA

was extracted using Mammalian Total RNA Miniprep kit (MilliporeSigma, Burlington, MA, USA) and RNAs from each group were pooled with equal amounts. Total RNA sequencing was conducted by Rhelixa Japan. RNA-Seq library was constructed, followed by next-generation sequencing on Illumina platform with total raw reads at 40 million per sample. The raw sequencing data were processed using Galaxy platform. The reads were trimmed by Trimmomatic, and then aligned by HISAT2 referred to genome GRCm38 (mm10). Data were transformed to log2 (TPM+1) for further analysis. Genes with fold change >1 or <1 were considered as upregulated and downregulated genes, respectively. Upregulated and downregulated genes were used for KEGG pathway analysis. Heatmaps were normalized by row and plotted using pheatmap R package and GraphPad Prism software. RNA-Seq raw and processed data were deposited in GEO repository with the accession number GSE190289.

Reverse transcription quantitative real-time PCR (RT-qPCR)

For the analysis of gene expression, RNA was isolated using Mammalian Total RNA Miniprep kit (MilliporeSigma). Then, RNA concentration was measured by NanoDrop 2000c (Thermo Scientific) and 50 ng of RNA was treated with a High-Capacity cDNA Reverse Transcription kit (Applied Biosystems, Waltham, MA, USA) to generate cDNA. Next, cDNA was diluted 20 times and used in RT-qPCR prepared with TB Green® Premix Ex Taq™ (Takara, Kusatsu, Japan). Data were calculated using $2^{-\Delta Ct}$ method and normalized to *Gapdh, Hprt or Actb*. The following primers were used:
Gapdh forward 5'-TTCACCACCATGGAGAAGGC-3',
Gapdh reverse 5'-GGCATGGACTGTGGTCATGA-3',
Hprt forward 5'-AGCTACTGTAATGATCAGTCAACG-3',
Hprt reverse 5'-AGAGGTCCTTTTCACCAGCA-3',
Actb forward 5'-CAATAGTGATGACCTGGCCGT-3',
Actb reverse 5'-AGAGGGAAATCGTGCGTGAC-3',
Il17a forward 5'-TTTAACTCCCTTGGCGCAAAA-3',
Il17a reverse 5'-CTTTCCCTCCGCATTGACAC-3',
Il1b forward 5'-CAACCAACAAGTGATATTCTCCATG-3',
Il1b reverse 5'-GATCCACACTCTCCAGCTGCA-3',
Il6 forward 5'-GAGGATACCACTCCCAACAGACC-3',
Il6 reverse 5'-AAGTGCATCATCGTTGTTCATACA-3',
Csf2 forward 5'-GGCCTTGGAAGCATGTAGAGG-3',
Csf2 reverse 5'-GGAGAACTCGTTAGAGACGACTT-3',
Il10 forward 5'-GCTCTTACTGACTGGCATGAG-3',
Il10 reverse 5'-CGCAGCTCTAGGAGCATGTG-3',
Ifng forward 5'-GAACTGGCAAAAGGATGGTGA-3',
Ifng reverse 5'-TGTGGGTTGTTGACCTCAAAC-3',
Tnf forward 5'-GCCTCCCTCTCATCAGTTCT-3',
Tnf reverse 5'-CACTTGGTGGTTTGCTACGA-3',
Clec1a forward 5'-ATGCAGGCCAAATACAGCAG-3',
Clec1a reverse 5'-CCAGAATACAGGCTTATGGTGGT-3'.

In vitro MOG restimulation

On day 7 after EAE induction, mice were euthanized and sacrificed by cervical dislocation. Inguinal and axillary LNs were excised and disrupted by the hard part of a syringe plunge. Cells were passed through 100 μm mesh and seeded in a 96 well plate (Iwaki, Japan) at 3×10^5 cells/200 μl/well in RPMI1640 medium containing 10% FCS, 1% β-mercaptoethanol, 100 U/ml penicillin, and 100 μg/ml streptomycin. MOG peptide at different final concentrations as shown was added, and cells were incubated at 37°C 5% CO_2 for 72 h. For cell proliferation analysis, [^{3}H]TdR (5 μCi/ml; PerkinElmer, Waltham, MA, USA) was incorporated for 10 h at the end of incubation, the radioactivity incorporated into acid-precipitable fraction was measured with a MicroBeta^2 RI counter (PerkinElmer), and presented as counts per min (cpm).

Co-culture of 2D2 Tg T cells and DCs

The spleen, mesenteric LNs, and dLNs were prepared from WT and 2D2 Tg mice and tissue was destroyed using a syringe plunge and filtered through 100 μm mesh. After treatment with hemolysis buffer (140 mM NH_4Cl and 17 mM Tris-HCl, pH 7.2), cells were treated with anti-CD16/CD32 antibody (2.4G2 Ab, produced in-house) to reduce non-specific binding. Next, Thy1.2$^+$ T cell were isolated using Thy1.2 microbeads with an autoMACS Pro separator (Miltenyi Biotec, Bergisch Gladbach, Germany). For isolation of DCs, WT or *Clec1a*$^{-/-}$ mouse spleens were treated with 2 U/ml LiberaseTM (MilliporeSigma) and 20 U/ml DNaseI (MilliporeSigma) for 30 min at 37°C in shaking water bath. Following hemolysis and CD16/CD32 blocking, DCs were collected by sorting CD11c$^+$ cells from splenocytes by depleting Thy1.2 and CD19$^+$ cells with an autoMACS Pro separator. T cells (2×10^5) and DCs (0.5×10^4) were co-cultured for two days in RPMI1640 medium containing 10% FCS, 1% β-mercaptoethanol, 100 U/ml penicillin, and 100 μg/ml streptomycin in the presence of MOG peptide at the indicated concentrations. After 48 h, [^{3}H] TdR was incorporated for 12 h, the radioactivity was measured with a MicroBeta^2 RI counter (PerkinElmer), and presented as cpm.

Preparation of single cells from organs

Single cell suspensions from dLNs were obtained by dissociating the tissue with a syringe plunge. For isolation of single cells, minced organs (spleen, lung) were treated with mixture of 2 U/ml LiberaseTM (Millipore-

Sigma) and 20 U/ml DNaseI (MilliporeSigma) in RPMI1640 medium containing 10% FCS, 1% β-mercaptoethanol, 100 U/ml penicillin, and 100 μg/ml streptomycin, for 30 min at 37°C water bath with shaking. Then the suspension was passed through sterile gauze and washed with FACS buffer (Hanks' Balanced Salt Solution containing 2% FCS).

Flow cytometry

Single cell suspensions from dLNs and spleen were prepared. Following hemolysis, cells were stained with specific antibodies at 1–2.5 μg/ml for 30 min at 4°C according to the manufacture's manual. After a wash in FACS buffer, samples were fixed with 4% paraformaldehyde overnight at 4°C. Then, samples were washed, diluted in FACS buffer, and analyzed by a BD FACSCanto™ II flow cytometer. FlowJo FACS software was used for flow cytometry data analysis.

Antibodies against CD3 (145-2C11) and CD19 (1D3) were obtained from BD Biosciences (Franklin Lakes, NJ, USA), and antibodies against CD45.2 (104), CD45.1 (A20), CD4 (GK1.5), CD8 (53-6.7), CD11c (N418), F4/80 (BM8), γδTCR (GL3), and MHC class II (M5/114.15.2) were obtained from BioLegend (San Diego, CA, USA), and antibodies against Foxp3 (FJK-16S) were obtained from eBioscience (San Diego, CA, USA).

Measurement of antibody (Ab) titer against MOG peptide

The titer of anti-$MOG_{35–55}$ antibodies was measured by ELISA as described [32]. Briefly, 96-well plates were coated with $MOG_{35–55}$ peptide (100 μg/ml in 40 μl per well) by incubating at 4°C overnight. Then, plates were washed with PBS-T (PBS containing 0.01% Tween20) three times and blocked by 1% BSA in PBS-T for 1 h at room temperature. After washing, 40 μl of 20-fold diluted sera were incubated in duplicates for 1 h at room temperature. Next, alkaline phosphatase-labeled goat anti-mouse Igs (SantaCruz Biotechnology, Dallas, TX, USA) were reacted for 1 h at room temperature, followed by the addition of p-nitrophenyl phosphate substrate (MilliporeSigma). The titer of anti-$MOG_{35–55}$ antibody is given as an absorbancy value at 405 nm.

Preparation of bone marrow-derived myeloid cells

Bone marrow (BM) was extracted from the tibia and femur, and red blood cells were eliminated using hemolysis buffer. Then, BM cells were cultured at 2×10^6 cells/ml in RPMI1640 supplemented with 10% FCS, 100 U/ml penicillin, 100 μg/ml streptomycin, 1% β-mercaptoethanol, and 50 ng/ml recombinant mouse Flt3L (Fms-like tyrosine kinase 3-ligand) (Peprotech, Cranbury, NJ, USA) for 10 days. Loosely adherent and non-adherent cells were collected on day 10.

For preparation of GM-CSF-induced DCs (GMDCs), BM cells were cultured at 2×10^5 cells/ml in RPMI1640 supplemented with 10% FBS, 100 U/ml penicillin, 100 μg/ml streptomycin, 1% β-mercaptoethanol, and recombinant mouse GM-CSF (20 ng/ml; Peprotech, Rocky Hill, NJ, USA) in non-treated dishes. Loosely adherent and non-adherent cells were collected on day 8.

For preparation of BM macrophages, BM cells were cultured at 2×10^6 cells/ml in RPMI1640 supplemented with 10% FBS, 100 U/ml penicillin, 100 μg/ml streptomycin, 1% β-mercaptoethanol, and recombinant human M-CSF (20 ng/ml; R&D Systems, Minneapolis, MN, USA). On day 7, adherent cells were collected by scraping with 2.5 mM EDTA/PBS.

Cell stimulation

For cell stimulation experiments, FL-DCs (1×10^6/well) were incubated in the presence of poly (I:C) (50 μM, InvivoGen, San Diego, CA, USA) or zymosan (100 μg/ml, MilliporeSigma) at 37°C for 24 h. Then, cells were analyzed by flow cytometry for specific cell activation markers.

For stimulation of spleen cells, spleens were cut and incubated with a mixture of 2 U/ml LiberaseTM (MilliporeSigma) and 20 U/ml DNaseI (MilliporeSigma) in RPMI1640 medium containing 10% FCS, 1% β-mercaptoethanol, 100 U/ml penicillin, and 100 μg/ml streptomycin, for 30 min at 37°C water bath with shaking. Then, the suspension was passed through sterile gauze and 5×10^5 cells in 200 μl were seeded in a 96-well plate. Indicated concentrations of LPS, PTX or *M. tuberculosis* were added in 10 μl of PBS. Polymyxin B (10 μg/ml) (MilliporeSigma) was added to all wells to exclude the influence of LPS in PTX or *M. tuberculosis* samples. After 16 h incubations cells were collected, and RNA was isolated using Mammalian Total RNA Miniprep kit (MilliporeSigma) with further RT-qPCR analysis.

Mixed lymphocyte reaction

Splenic $CD4^+$ and $CD8^+$ T cells from BALB/cA mice were sorted by autoMACS Pro separator. WT and *Clec1a*$^{-/-}$ FL-DCs ($CD24^+$ or $CD11b^+$) from C57BL/6 mice were sorted by BD FACSAria II. Then, 2×10^5 T cells were co-cultured with DCs at indicated ratios for three days. Then, T cell proliferation was assessed by [^{3}H]TdR incorporation, the radioactivity was measured with a MicroBeta^2 RI counter (PerkinElmer), and presented as cpm.

Statistics

Data were analyzed using the GraphPad Prism software (La Jolla, CA, USA). Statistical analysis was performed using Student's *t*-test except for the disease score and Igs ELISA. Mann-Whitney *U* test was used to determine statistical significance of disease score. Welch's *t* test was used for analysis of Igs. Differences of $P<0.05$ were considered statistically significant. Data are presented as mean ± SD.

Results

Generation of *Clec1a*$^{-/-}$ mice

Clec1a$^{-/-}$ mice were generated by deleting the exon I using homologous recombination techniques in a C57BL/6N-derived ES cell (Supplementary Fig. 1A). Homologous recombination was confirmed by Southern blot hybridization analysis and genotypes were determined by PCR (Supplementary Fig. 1B and C). The *Clec1a* gene expression was completely disappeared in homozygous deficient mice (Supplementary Fig. 1D). Homozygous *Clec1a*-deficient mice were normally born at the Mendelian ratio from heterozygous parents, grew healthy, and were fertile. No apparent abnormalities were observed at least one year of age.

We observed relatively high *Clec1a* expression in the lung, heart, and LNs under physiological conditions (Fig. 1A). High levels of *Clec1a* expression were observed in CD31$^+$ endothelial cells (Fig. 1B), consistently with the observation by Stappers *et al.* [36]. Low, but significant levels of expression were observed in CD11c$^+$ DCs and CD11b$^+$ monocytes. Furthermore, *Clec1a* expression level was measured in BM-derived myeloid cells, including DCs generated from BM cells by treating with 50 ng/ml Flt3L for 10 days (FL-DCs), DCs generated from BM cells by treating with 20 ng/ml GM-CSF for 8 days (GMDCs), and BM-derived macrophages (BMMs), generated by culture of BM cells in presence of 20 ng/ml M-CSF. Relatively high level of *Clec1a* expression was detected in CD24$^+$ FL-DCs, which represents cDC1, in comparison to CD11b$^+$ FL-DCs, which represents cDC2, or GMDCs and BMMs (Fig. 1C). The composition of immune cells such as T cells and B cells was normal in these *Clec1a*$^{-/-}$ mice (Fig. 1D). Additionally, the amount of naïve (CD44$^-$CD62L$^+$) and memory (CD44$^+$CD62L$^-$) T cells was similar between WT and *Clec1a*$^{-/-}$ mice, as well as the expression of an activation marker CD69 in CD44$^+$ or CD62L$^+$ T cells (Fig. 1E). Furthermore, the content of total CD11c^{hi} and MHCII^{hi} DCs, resident DCs (CD11c^{hi} DCs), and migratory DCs (MHCII^{hi} DCs) in axillary and inguinal LNs in *Clec1a*$^{-/-}$ mice were comparable to WT mice (Fig. 1F).

Development of EAE is suppressed in *Clec1a*$^{-/-}$ mice

Next, we examined possible involvement of Clec1A in the development of EAE. We found that the disease score estimated by the levels of paralysis of the tail and legs was lower in *Clec1a*$^{-/-}$ mice than that in WT mice, although the difference was not always statistically significant (Fig. 2A, B, and Supplementary Fig. 2). As shown in Fig. 2B and Supplemetary Fig. 2, the development of EAE was statistically significantly suppressed in 5 experiments in total 8 independent trials with similar tendency in the rest of experiments. In this significantly suppressed experiment shown in Fig. 2B, mean maximum score was lower in *Clec1a*$^{-/-}$ mice than that in WT mice (Fig. 2C), but average disease onset day was similar between these mice (Fig. 2D). Histological examination revealed that inflammatory cell infiltration was significantly suppressed in *Clec1a*$^{-/-}$ mice compared to WT mice (Fig. 2E). Demyelination of the spinal cord assessed by LFB staining was also significantly suppressed in *Clec1a*$^{-/-}$ mice compared with WT mice, consistent with the neurological symptoms (Fig. 2F). These results show that EAE development is suppressed in *Clec1a*$^{-/-}$ mice.

Cell composition in the spleen and dLNs after EAE induction is similar between *Clec1a*$^{-/-}$ mice and WT mice

Cell composition was checked at two time points after EAE induction: 1) before development of EAE symptoms (day 10), and 2) at the peak of the disease (day 16). As shown in Fig. 3, the proportion of CD4$^+$, CD8$^+$ T, and B (CD19$^+$) cells in the spleen (Fig. 3A) and axillary and inguinal dLNs (Fig. 3B) was comparable between WT and *Clec1a*$^{-/-}$ mice at day 10 and 16 after EAE. However, CD19$^+$ B cell percentage was slightly decreased in *Clec1a*$^{-/-}$ mice at day 16 in spleen (Fig. 3A). The proportion of F4/80$^+$ macrophages, CD11b$^+$ myeloid cells, and CD11c$^+$ DCs were low in the dLNs at day 10 after EAE induction, but significantly increased at day 16 in both WT and *Clec1a*$^{-/-}$ mice (Fig. 3B), although the increase of F4/80$^+$ cells, CD11b^{hi} cells, and CD11c$^+$ cells was not observed in the spleen (Fig. 3A). MHCII$^+$ CD11c$^+$ DCs were marginally decreased in *Clec1a*$^{-/-}$ mice compared with WT mice at day 10 and slightly increased in the draining LNs at day 16 (Fig. 3B).

Recall memory T cell proliferation is decreased in *Clec1a*$^{-/-}$ mice after immunization with MOG peptide while Ab production against MOG peptide is normal

As demyelination of the spinal cord was likely to be caused by the T cell-mediated immune response against

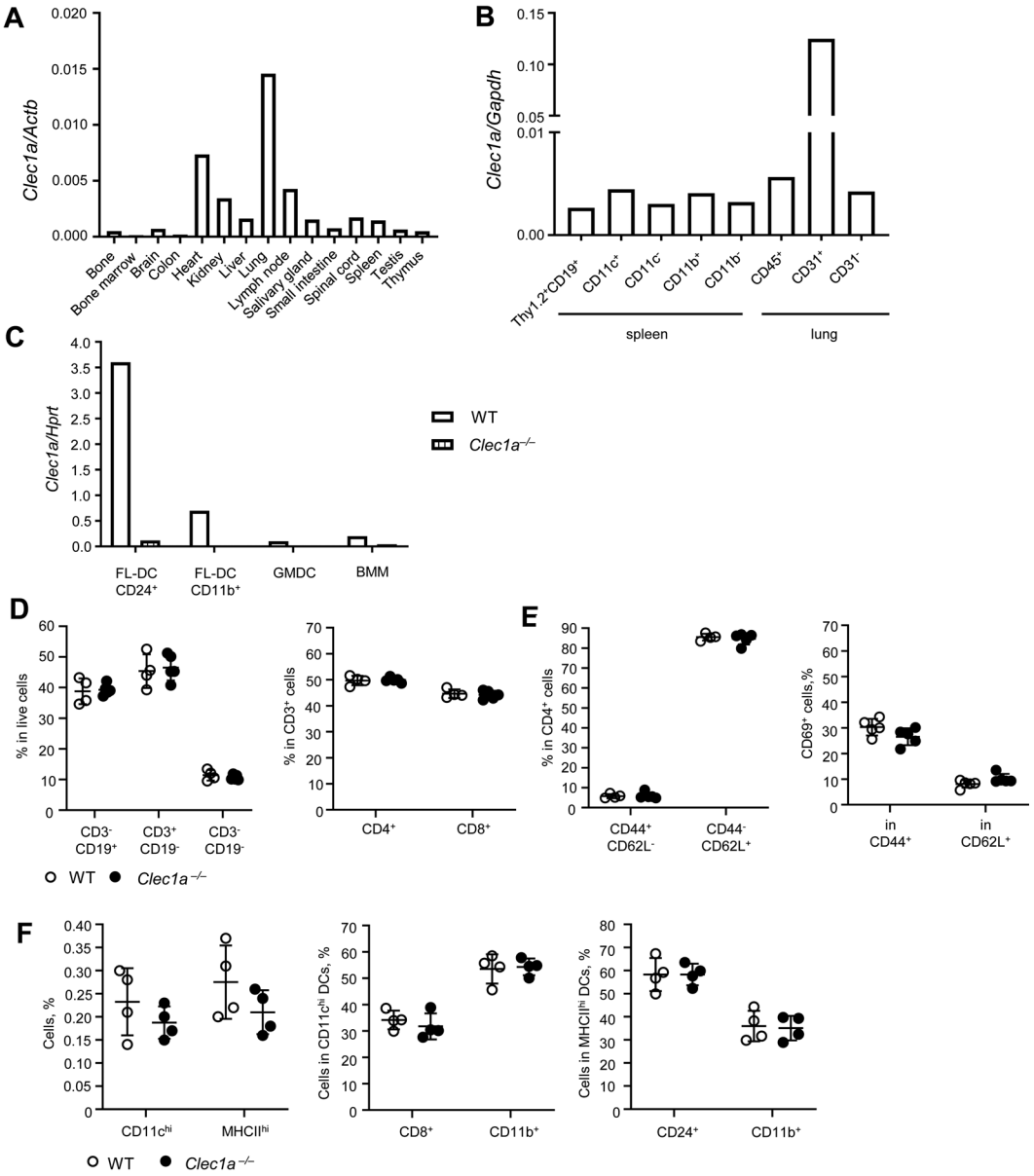

Fig. 1. Tissue specificity of *Clec1a* expression under physiological conditions. A. Tissue specific expression of *Clec1a* was examined using RT-qPCR. The expression levels relative to β-actin expression are shown. B. Splenocytes were separated into $CD11c^+$ cells and $CD11b^+$ cells after sorting out the mixture of T and B cells by MACS. Also, dissociated lung cells were separated into $CD45^+$ cells and $CD45^-$ cells, and $CD45^-$ fraction was further separated into $CD31^+$ cells and $CD31^-$ cells. Then, *Clec1a* expression in these cell populations was analyzed by RT-qPCR. C. *Clec1a* expression was measured by RT-qPCR in BM-derived cells including FL-DCs ($CD24^+$ and $CD11b^+$), GM-DCs, and BMMs. FL-DCs were sorted by BD FACSAria II. D. Immune cell composition in the spleen was compared between WT and *Clec1a*$^{-/-}$ mice using flow cytometry. $CD3^-CD19^+$, $CD3^+CD19^-$ and $CD3^-CD19^-$ cells (left panel). $CD4^+$ cells and $CD8^+$ cells in $CD3^+$ cells (right panel). E. $CD44^+CD62L^-$ cells and $CD44^-CD62L^+$ cells in $CD4^+$ cells (left panel). $CD69^+$ cells in $CD44^+$ cells and $CD62L^+$ cells (right panel). F. DC content in inguinal and axillary LN cells was analyzed by flow cytometry. $CD11c^{hi}$ and $MHCII^{hi}$ populations (left panel). $CD8^+$ and $CD11b^+$ cells in $CD11c^{hi}$ DCs (center panel). $CD24^+$ and $CD11b^+$ cells in $MHCII^{hi}$ DCs (right panel).

MOG [44], we examined recall memory T cell proliferation against MOG peptide. Draining LN cells were prepared from MOG peptide-immunized mice at day 7 after EAE induction before the development of the symptoms, and T cell proliferative response against MOG peptide was examined by [^{3}H]TdR incorporation (Fig. 4A and Supplementary Fig. 3A–H). [^{3}H] incorporations were reduced in LN cells from *Clec1a*$^{-/-}$ mice compared with WT mice, although significant reduction was observed only in 4 experiments out of 9 independent trials (Fig. 4B and Supplementary Fig. 3A–H). These results suggest that T cell sensitization was impaired in *Cle-*

 doi: 10.1538/expanim.21-0191

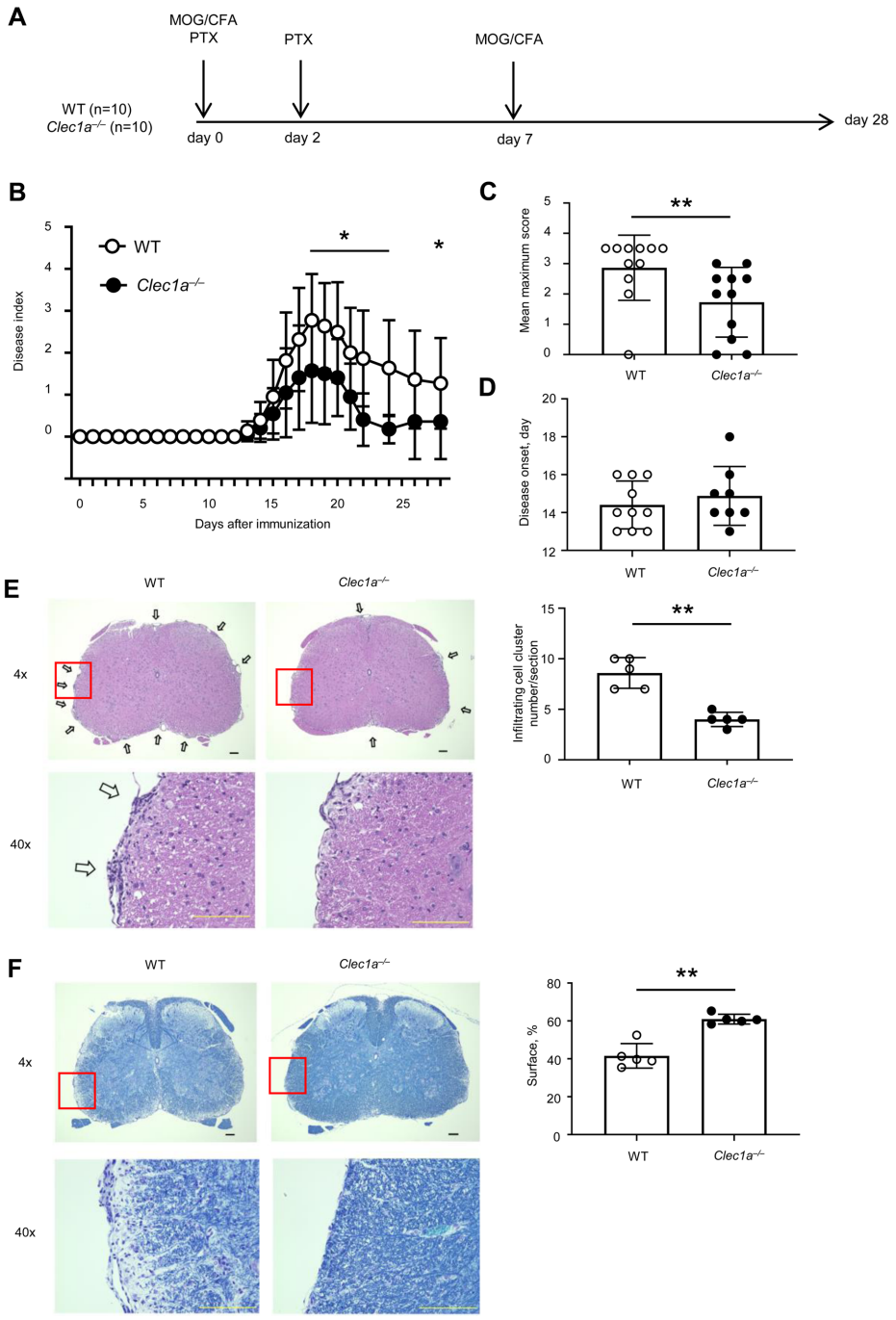

Fig. 2. Development of EAE is suppressed in *Clec1a*$^{-/-}$ mice. A. Schematic presentation of the induction of EAE. WT (n=10) and *Clec1a*$^{-/-}$ (n=10) mice were immunized with MOG peptide in CFA s.c. and PTX was injected i.p. on the same day. On day two, second PTX was injected. Then, on day seven, immunization with MOG peptide in CFA was repeated. Mice were sacrificed on day 28 and analyzed histologically. B. Mean clinical score of WT (white circle) and *Clec1a*$^{-/-}$ (black circle) mice were measured every day by assessing tail and limbs paralysis. The figure shows representative of total 8 independent experiments with similar results, in which 5 of the experiments showed significant difference. The data of the other 7 experiments are shown in Supplementary Fig. 2. Statistical significance was calculated by Mann-Whitney *U* test. **P*<0.05. C. Mean maximum disease score of WT and *Clec1a*$^{-/-}$ mice shown in B. Statistical significance was calculated by Mann-Whitney *U* test. ***P*<0.01. D. Average onset day of WT and *Clec1a*$^{-/-}$ mice shown in B. E. Histological analysis of the spinal cord of EAE-induced mice. Left panels. On day 28, a half of the mice shown in B (n=5 for each) were sacrificed, and the spinal cords were excised, formalin fixed, and sections (10 μm) were stained with H & E. Then, the tissue sections were inspected with ×4 (upper) and ×40 (lower) objectives (left panels). Scale bar represents 100 μm. Arrows show the sites where inflammatory cells infiltrate. The images were analyzed by ImageJ software and quantified the number of infiltrating cell clusters. Average of infiltrating cell cluster number/ section is shown. The figures show representative of 5 mice for each. Statistical significance was calculated by Mann-Whitney *U* test. ***P*<0.01. F. The same spinal cord samples used in E were used for LFB staining. Left panels: the same spinal cord sections as C were stained with LFB and photos were taken under a microscope. The tissue sections were inspected with ×4 (upper) and ×40 (lower) objectives (left panels). Scale bar represents 100 μm. Right panel: LFB stained area was measured using ImageJ software. The figures show representative of 5 mice for each. Statistical significance was calculated by Mann-Whitney *U* test. ***P*<0.01.

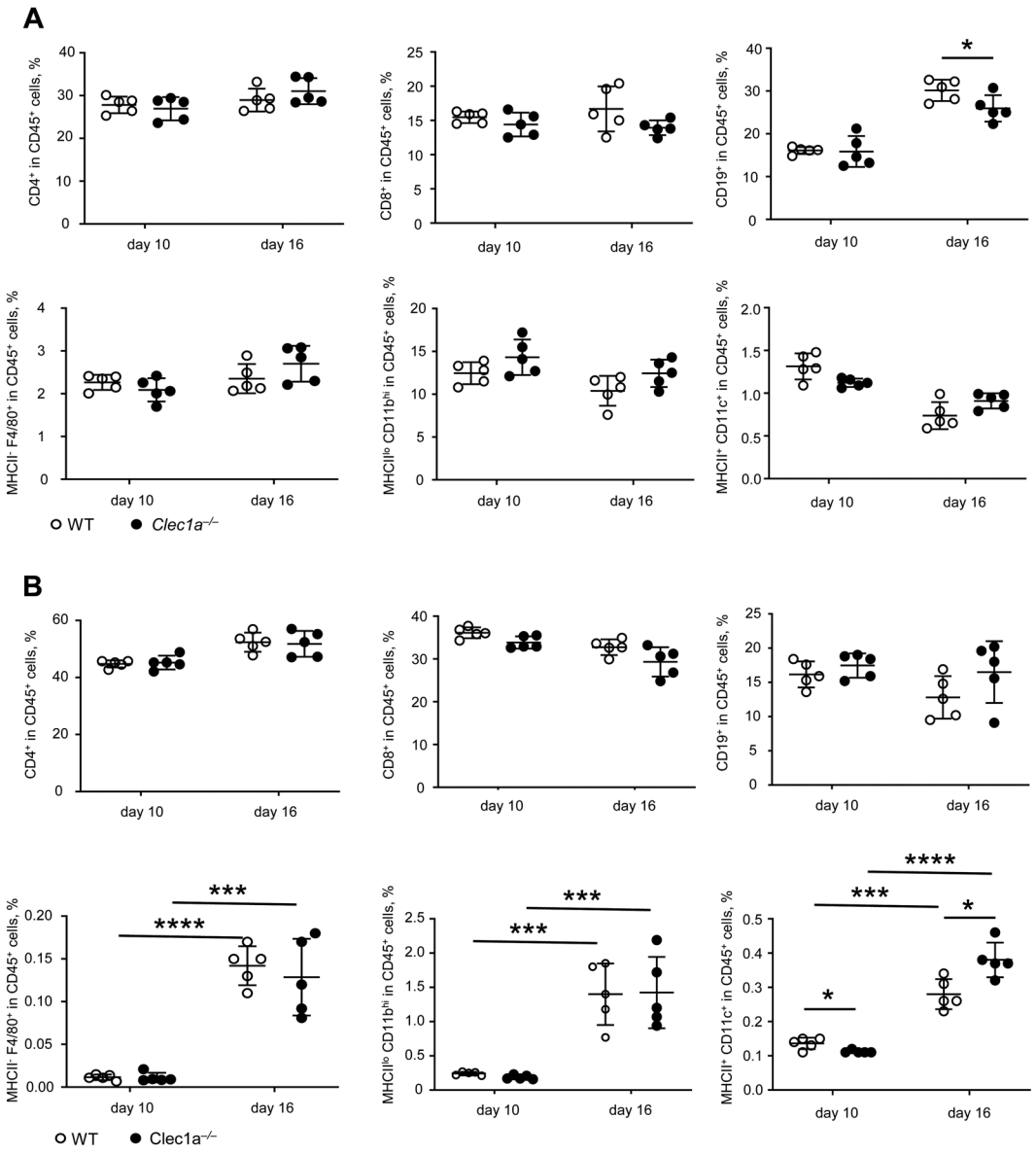

Fig. 3. Immune cell compositions of the spleen and inguinal and axillary LNs are comparable between WT and *Clec1a*$^{-/-}$ mice. Spleen (A) and dLN (B) cell populations were analyzed on day 10 and day 16 after EAE induction for WT (n=5, white circle) and *Clec1a*$^{-/-}$ (n=5, black circle) mice. The result from one experiment shown in Supplementary Fig. 2D is presented. Statistical significance was calculated by Student's *t* test. **P*<0.05, ****P*<0.001, *****P*<0.0001.

c1a$^{-/-}$ mice compared with WT mice.

Next, we examined antibody production against MOG after EAE induction. The disease score graph of this experiment is presented on Fig. 2B. We found that similar levels of Abs were detected in the serum of both WT and *Clec1a*$^{-/-}$ mice (Fig. 4C). These observations suggest that antibody production against MOG peptides is normal in *Clec1a*$^{-/-}$ mice.

DC cell differentiation is normal in *Clec1a*$^{-/-}$ mice while antigen-presenting ability of DCs is moderately decreased

Next, we examined the differentiation and antigen-presenting ability of *Clec1a*$^{-/-}$ mouse DCs. First, we induced DC differentiation from BM cells by treating with 50 ng/ml Flt3L for 10 days (FL-DCs), which is reported to include cDC-like populations [45]. CD24^{+}, which represents cDC1, as well as CD11b^{+}, which represents cDC2, FL-DCs were normally differentiated from both WT and *Clec1a*$^{-/-}$ BM cells (Fig. 5A). Expression of cell surface markers for maturation and activation state of DCs, such as I-A/I-E, CD80 and CD86, was comparable between WT and *Clec1a*$^{-/-}$ FL-DCs (Fig. 5B). Furthermore, the expression of I-A/I-E, CD80 and CD86 after stimulation with zymosan or Poly (I:C) was also similar (Fig. 5C). In addition, cytokine gene expres-

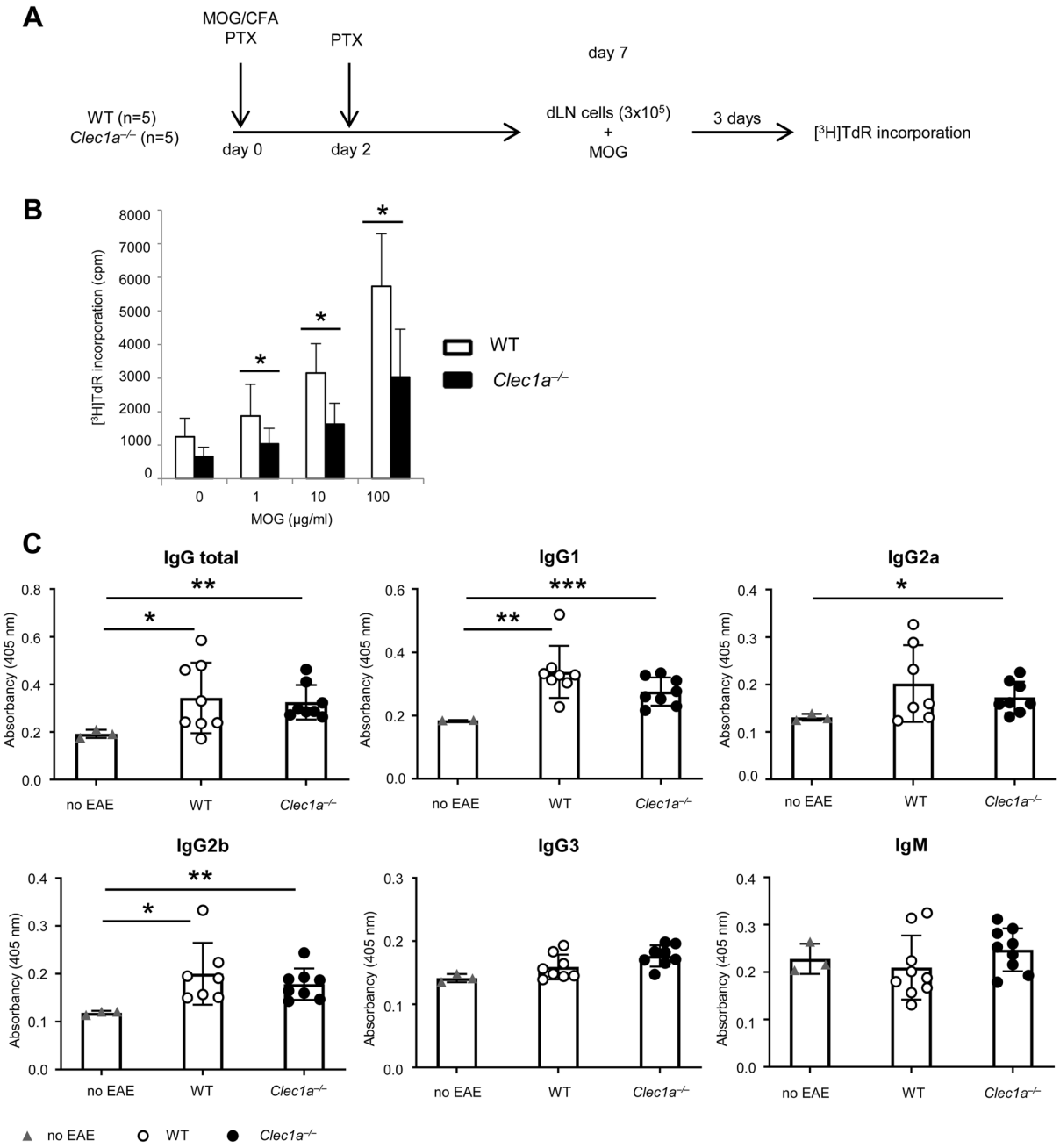

Fig. 4. Recall memory T cell proliferation of *Clec1a*$^{-/-}$ mice is decreased upon *in vitro* restimulation with MOG peptide. A. Schematic presentation of T cell restimulation experiments after induction of EAE. WT (pooled, n=5) and *Clec1a*$^{-/-}$ (pooled, n=5) mice were immunized with MOG peptide according to the standard protocol. On day seven after induction of EAE, draining LNs were collected, and cells (3×10^5) were stimulated *in vitro* with indicated concentrations of MOG peptide. After three days incubation, cells were treated with [^{3}H]TdR for 12 h, and acid precipitable radioactivity was measured. B. MOG peptide-dose-dependent [^{3}H]TdR incorporations were compared between T cells from WT and *Clec1a*$^{-/-}$ mice. Four well replicates were counted. The results with similar tendency were reproduced in 6 experiments out of total 9 experiments, but significant difference was observed only in 4 experiments. These data are shown in Supplementary Fig. 3. Statistical significance was calculated by Student's *t* test. **P*<0.05. C. Ab titer in serum against MOG of each Ig subtype was measured at day 28 after induction of EAE. WT mice without EAE induction (no EAE): n=2 or 3; WT mice after EAE induction: n=7; *Clec1a*$^{-/-}$ mice after EAE induction: n=8. The result is representative of 2 independent experiments. Statistical significance was calculated by Student's *t* test. **P*<0.05, ***P*<0.01, ****P*<0.001.

sion levels were analyzed after stimulation of spleen cells with LPS, PTX, and *M. tuberculosis*. We found that the expression levels of *Il6* and *Tnf* were similar between *Clec1a*$^{-/-}$ mouse-derived cells and WT mouse-derived cells (Fig. 5D).

Next, antigen-presenting ability of these FL-DCs was examined. For this, we performed mixed lymphocyte culture using these BMDCs from C57BL/6 background

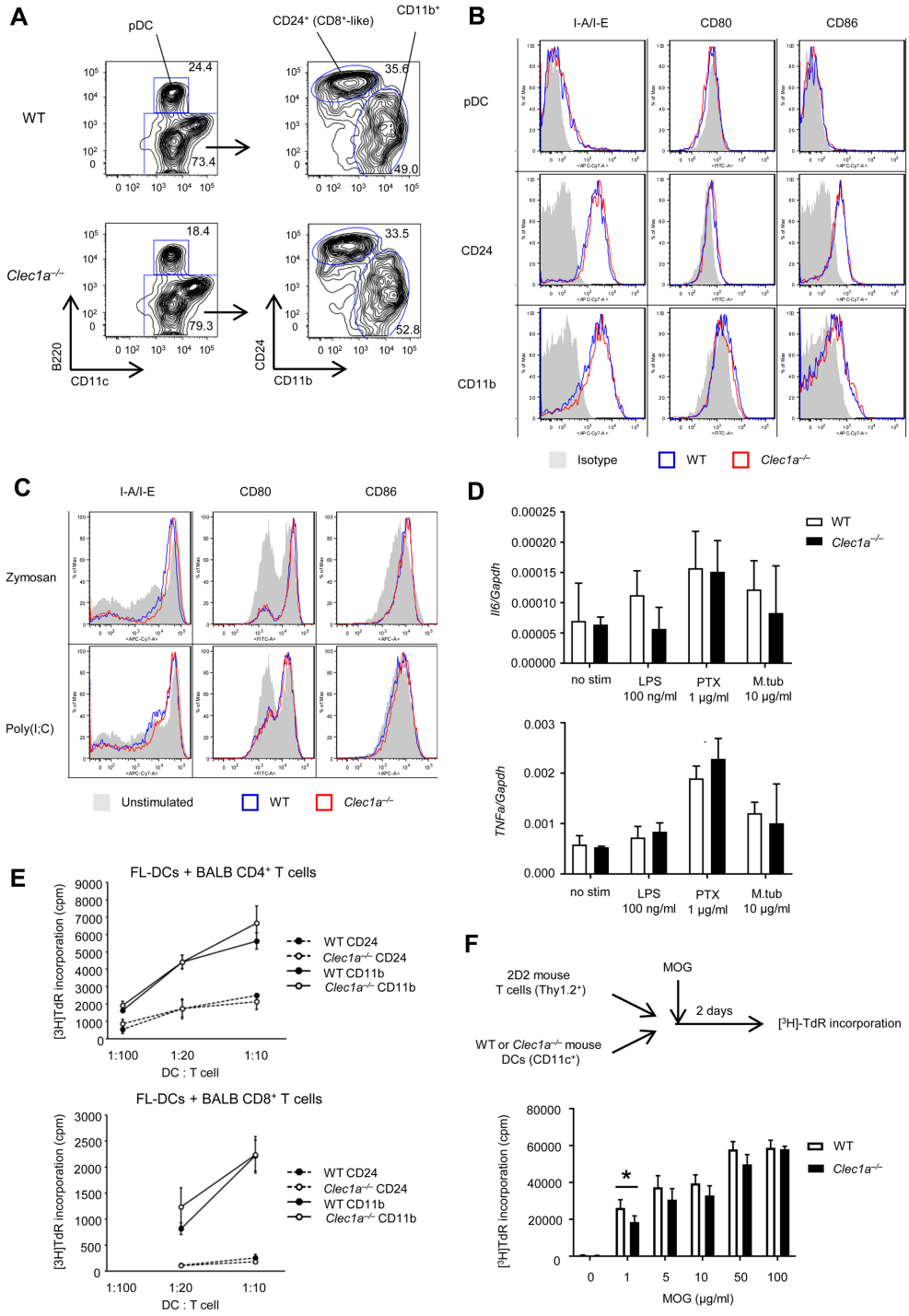

Fig. 5. DC differentiation is normal in *Clec1a*$^{-/-}$ mice while antigen-presenting ability of DCs is moderately decreased. A. FL-DCs were induced to differentiate from BM cells with 50 ng/ml Flt3L for 10 days, and CD11c^{+}B220^{+} (pDC) cells and CD24^{+}CD11b^{-} (CD8^{+}-like) and CD11b^{+}CD11c^{+} cells were analyzed by FACS. B. Cell surface markers including I-A/I-E, CD80 and CD86 on FL-DCs (pDC, CD24^{+} and CD11b^{+} cells) were examined by FACS. C. Cell surface markers were examined after stimulation with zymosan and poly (I:C). D. The expression of *Il6* (upper) and *Tnf* (lower) was measured by RT-qPCR after stimulation of splenic cells with LPS, PTX, or *M. tuberculosis* (M.tub) at designated concentrations. Polymyxin B (10 μg/ml) was added to all samples. The result is representative of 2 independent experiments. E. Antigen presenting ability of C57BL/6J FL-DCs (2×10^5 cells) was examined by allogeneic mixed lymphocyte response with increased number of BALB/c mouse-derived CD4 cells or CD8 cells. T cell proliferative response was measured by [^{3}H]TdR incorporation. F. Antigen-presenting ability of DCs from *Clec1a*$^{-/-}$ mice was examined using MOG-specific 2D2 Tg T cells. Upper panel: Schematic presentation of 2D2 Tg T cell stimulation experiments after co-culture with DCs in the presence of MOG. WT (pooled, n=5) and *Clec1a*$^{-/-}$ (pooled, n=5) mouse splenic CD11c^{+} DCs (5×10^3 cells/100 μl) were cultured together with 2D2 Tg mouse Thy1.2^{+} T cells (2×10^5 cells/100 μl) in the presence of increasing concentrations of MOG peptide. After two days, cells were treated with [^{3}H]TdR for 12 h, and acid precipitable radioactivity was measured. Lower panel: [^{3}H]TdR incorporations are shown. DCs from WT mice: white bars, *Clec1a*$^{-/-}$ mice: black bars. Four well replicates were counted. The figure shows representative of two individual experiments. The second experiment graph is showed in Supplementary Fig. 3I. Statistical significance was calculated by Student's *t* test. **P*<0.05.

mice. When $CD24^+$ or $CD11b^+$ FL-DCs were cocultured with BALB/c mouse-derived $CD4^+$ and $CD8^+$ T cells, allogeneic MHC-stimulated T cell proliferation was similar between WT and *Clec1a*$^{-/-}$ mouse-derived FL-DCs (Fig. 5E).

Furthermore, we examined antigen-presenting ability of *Clec1a*$^{-/-}$ DCs against MOG peptide. $Thy1.2^+$ cells were isolated from spleens and dLNs of 2D2 Tg mice, which express a transgenic MOG-specific T cell receptor, and $CD11c^+$ DCs were purified from the spleen cells of WT or *Clec1a*$^{-/-}$ mice by MACS. Then, 2D2 Tg T cells and DCs from either WT or *Clec1a*$^{-/-}$ mice were cocultured in presence of various concentrations of MOG peptide (Fig. 5F). T cell proliferation was measured by [^{3}H]TdR incorporation after three-day-culture. We found that T cell proliferation tended to be lower with *Clec1a*$^{-/-}$ mouse DCs than that with WT DCs as the antigen-presenting cells (Fig. 5F). These results together with the results shown in Fig. 4B suggest that antigen-presenting ability of DCs of *Clec1a*$^{-/-}$ mice is impaired.

Inflammatory cytokine gene expression is reduced in *Clec1a*$^{-/-}$ mice

Next, gene expression in *Clec1a*$^{-/-}$ mice was examined by RNA-seq analysis. Inguinal dLNs were collected from WT and *Clec1a*$^{-/-}$ mice in a steady-state as well as after EAE induction at day 10 and day 16. The disease score graph of this experiment is presented on Supplementary Fig. 2D. As shown in Fig. 6, expression levels of 506 genes were up-regulated while 399 genes were decreased in *Clec1a*$^{-/-}$ mice even under physiological conditions (Fig. 6A). After induction of EAE, expression levels of 471 genes were increased and 391 genes demonstrated down-regulation in *Clec1a*$^{-/-}$ mice at day 10 (Fig. 6A). At day 16, 470 genes expression level were increased and at the same time 487 genes were decreased in *Clec1a*$^{-/-}$ mice (Fig. 6A).

Then, KEGG pathway database was used for analysis of pathways that were different between WT and *Clec1a*$^{-/-}$ mice. Several pathways, including IL-17 signaling pathway, TNF signaling pathway, chemokine signaling pathway, and inflammation-associated signaling pathways were attenuated in *Clec1a*$^{-/-}$ mice on day 10 after EAE induction even before onset of the neurological symptoms (Fig. 6B). Interestingly, only minor pathways were affected in a steady-state and on day 16, when the symptoms were most severe (Supplementary Fig. 4A).

According to the pathway analysis, we compared the expression of cytokines, chemokines, and transcription factors of these genes (Fig. 6C, Supplementary Fig. 4B, and C). We found that the expression levels of *Il23a, Il15,* and *Foxp3* were low in *Clec1a*$^{-/-}$ mice in a steady-state, while those of *Il4*, *Il5*, and *Tslp* were higher compared to WT mice. Interestingly, the expression of inflammatory cytokines such as *Il17a*, *Il6* and *Il1β*, was substantially increased in WT mice, but not in *Clec1a*$^{-/-}$ mice, at day 10 before the development of symptoms. In contrast, the difference was marginal at day 16 after development of paralysis (Fig. 6C, Supplementary Fig. 4B, and C). The expression of several chemokines such as *Ccl2*, *Ccl7*, *Cxcl1*, *Cxcl2* and *Cxcl10* was similarly significantly decreased in *Clec1a*$^{-/-}$ mice at day 10 compared to WT mice (Fig. 6C). On the other hand, the expression of genes such as *Il20*, *Irf2*, *Il4, Il21,* and *Rora*, was rather higher in *Clec1a*$^{-/-}$ mice than WT mice (Fig. 6C and Supplementary Fig. 4B). Interestingly, at day 16, inflammatory cytokine gene expression was already leveled off. We confirmed these results by RT-qPCR analyses using the same samples and independently prepared RNA samples, although the difference was not statistically significant in the latter experiment (Fig. 6D and Supplementary Fig. 5).

Discussion

In this report, we have first shown that the development of EAE is suppressed in *Clec1a*$^{-/-}$ mice compared with WT mice, indicating a novel function of Clec1A. Clec1A is highly expressed in $CD31^+$ endothelial cells and lower levels in myeloid cells. DC content and other immune cell contents were normal in dLNs and the spleen under physiological conditions, as well as on day 10 and day 16 after EAE induction. Myeloid cells such as $F4/80^+$ macrophages, $CD11b^+$ myeloid cells and $MHCII^+$ $CD11c^+$ DCs, but not of $CD4^+$ and $CD8^+$ T cells, were similarly increased at day 16 compared to day 10 in the draining LNs of both WT and *Clec1a*$^{-/-}$ mice. No abnormality in DC cell differentiation induced by Flt3L was observed. Gene expression of *Il6* and *Tnf* in *Clec1a*$^{-/-}$ mouse splenocytes after stimulation with PTX or *M. tuberculosis* was similar to that in WT mouse cells. Furthermore, antibody production against MOG peptide was also similar between WT and *Clec1a*$^{-/-}$ mice. However, we found that recall memory T cell proliferation after *in vitro* restimulation of T cells from EAE-induced mice with MOG peptide was reduced in cells from *Clec1a*$^{-/-}$ mice, suggesting T cell priming was impaired in *Clec1a*$^{-/-}$ mice. MOG-specific 2D2 Tg T cell proliferation upon stimulation with MOG peptide in the presence of *Clec1a*$^{-/-}$ DCs was also reduced, suggesting that antigen-presenting ability of DCs was impaired in these mutant mice. These observations indicate that antigen-presenting ability of DCs is impaired in *Clec1a*$^{-/-}$ mice, resulting in the insufficient T cell priming against MOG.

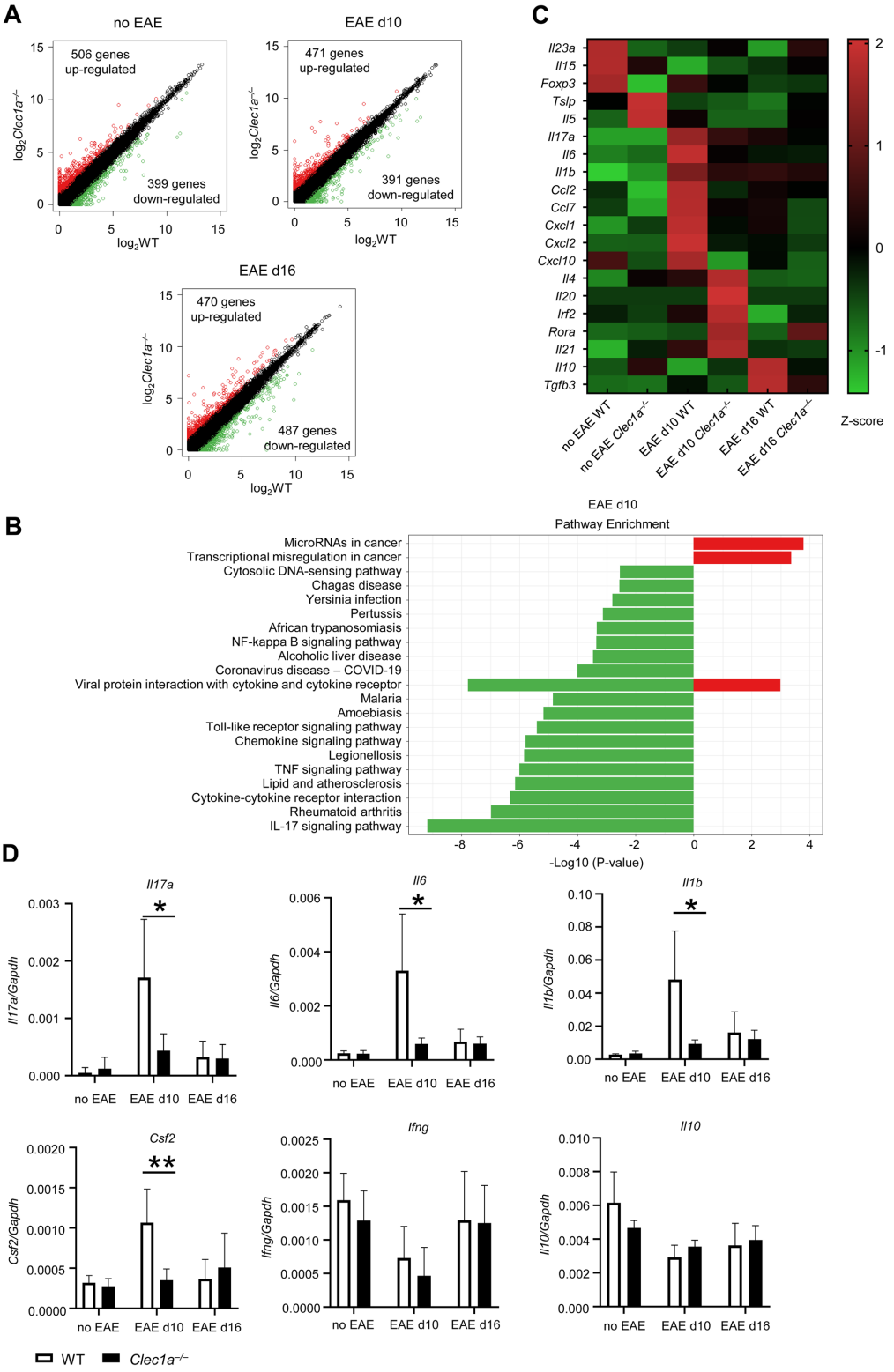

Fig. 6. Inflammatory cytokine gene expression in draining LNs is decreased in *Clec1a*$^{-/-}$ mice at day 10 after EAE induction. RNA expression in dLNs was analyzed by RNA-Seq in steady-state (before EAE induction), before the onset of the disease (day 10), and at the peak of the symptoms (day 16). Mice from the experiment shown in Supplementary Fig. 2D were used for the analysis. Draining LNs cells from 5 mice were pooled for each genotype and mRNA was extracted for the RNA-seq analysis. A. Number of up (red)- and down (green)-regulated genes detected by RNA-Seq and selected as differentially expressed genes (|log 2 (TPM+1)|>1, where TPM is transcript per million) between WT and *Clec1a*$^{-/-}$ mice at steady state, EAE d10 and EAE d16. B. KEGG pathway analysis of up- and down-regulated genes in *Clec1a*$^{-/-}$ mouse dLNs at day 10 EAE. C. Heatmap of mostly changed genes at different time points. Z-scores were computed for genes that are differentially expressed (|log 2 (TPM+1)|>1) between WT and *Clec1a*$^{-/-}$ mice and are presented as a heatmap. D. Gene expression of cytokines was examined by RT-qPCR in experiment that is shown in Supplementary Fig. 2D. Second independent experiment result is shown in Supplementary Fig. 5, and its disease score graph is shown in Supplementary Fig. 2E. Statistical significance was calculated by Student's *t* test. **P*<0.05, ***P*<0.01.

We have generated *Clec1a*$^{-/-}$ mice using C57BL/6N-derived ES cells and these mice were backcrossed for 2 generations to C57BL/6J mice, and we used C57BL/6J mice as the control. It was reported that C57BL/6N mice and C57BL/6J mice have some differences in immune-related genes [46, 47]; C57BL/6J mice have a defect in recruiting neutrophils to inflammatory sites compared with C57BL/6N mice due to a missense mutation in the *Nlrp12* gene. However, because *Clec1a*$^{-/-}$ mice developed milder EAE than that observed in C57BL/6J WT mice, this phenotype cannot be explained by the effect of this mutation in the control mice. Thus, we consider that the phenotype that we observed in *Clec1a*$^{-/-}$ mice is not caused by the difference of the genetic background, but caused by the *Clec1a* mutation itself.

We observed significant suppression of recall memory T cell proliferation only in 4 experiments out of 9 experiments (Supplementary Fig. 3). However, because T cell response of *Clec1a*$^{-/-}$ mouse-derived T cells was always lower than that of WT T cells, we considered that T cell response was impaired in the mutant mice. 2D2 Tg T cell proliferation suppression was also observed in only one of two experiments. Regarding these results, significant suppression of the development of EAE was also observed only 5 times in 8 experiments, although the development tended to reduce in other 3 experiments (Supplementary Fig. 2). Therefore, it is possible that we could not detect significant difference in recall memory T cell proliferation because EAE developments were not significantly different between *Clec1a*$^{-/-}$ mice and WT mice in these experiments, although the symptoms of EAE did not develop yet at day 7 after MOG immunization when dLN cells were prepared. We also could not detect any abnormalities in T cell proliferation in mixed lymphocyte culture and antibody production against MOG. These observations suggest that the effect of Clec1A-deficiency on DC function is only marginal, reflecting low levels of the expression of *Clec1a* in DCs.

We found that cytokine expression such as IL-17A, IL-6, and IL-1β, which are known to play important roles in the development of EAE, was greatly reduced in *Clec1a*$^{-/-}$ mice at day 10 after EAE induction. Decreased inflammatory cytokine expression was not a result of EAE suppression, because any symptoms did not yet develop at day 10. Enhanced cytokine expression was no more observed at day 16, when the paralysis was maximum. Thus, we conclude that reduced cytokine production is not a result but the cause for the impaired EAE development in *Clec1a*$^{-/-}$ mice.

Several groups including our group indicated that IL-17A plays an important role in the development of EAE, because EAE development is suppressed in *Il17a*-deficient mice [48, 49]. CCR6^{+}Th17 cells can cross the blood-brain barrier by an active transport mechanism involving the interaction with the CCL20^{+} 5th lumbar cord [11]. MOG-specific Th17 cells produce IL-17A by reacting to the myelin sheath of the nerve, and IL-17A induces production of inflammatory cytokines such as IL-1β, TNF, and IL-6, and recruits neutrophils through induction of chemokines CXCR2, causing inflammation in the CNS [50].

Cytokines such as IL-6, IL-1β and TGF-β can promote the differentiation of Th17 cells from naïve T cells [51, 52]. IL-23 + IL-1β directly induce *Il17a* expression in γδ T cells [8, 53], which are also involved in the early phase pathogenesis of EAE [7, 8]. Furthermore, components of *M. tuberculosis,* such as trehalose-6,6-dimycolate, induce Th17 cell differentiation through induction of cytokines, such as IL-1β, IL-6 and IL-23, via activation of the FcRγ-Syk-Card9 pathway [54]. PTX is also known to induce IL-1β and IL-6 by activating TLR4 on myeloid cells [55, 56].

Two possibilities are conceivable for the involvement of Clec1A in the development of EAE and associated cytokine production. One is that cytokine production in myeloid cells or endothelial cells after treatment with *M. tuberculosis* and PTX is impaired in *Clec1a*$^{-/-}$ mice. The other is that cytokine production induced by MOG-specific T cell response is reduced in *Clec1a*$^{-/-}$ mice. Regarding the former possibility, it seemed possible that cytokine production after treatment with *M. tuberculosis* and PTX is reduced in *Clec1a*$^{-/-}$ mice. This is because, upon treatment with stimulants such as LPS or IL-1β, cytokine and chemokine production are induced not only in myeloid cells but also in endothelial cells in which Clec1A is highly expressed [57, 58]. Thus, we tried to purify endothelial cells from *Clec1a*$^{-/-}$ mouse brain and lungs to examine the cytokine production after treatment with *M. tuberculosis* and PTX, but unfortunately, preparation of intact endothelial cells was quite difficult for us, and we could not examine cytokine production from endothelial cells. However, we consider this former possibility less likely, because initial cytokine production induced by these adjuvants should have finished by day 10 after EAE induction, when we observed the cytokine expression. Furthermore, the expression of *Il6* and *Tnf* in spleen cells after treatment of LPS, PTX or *M. tuberculosis* was similar between *Clec1a*$^{-/-}$ mice and WT mice.

Regarding the latter possibility, we showed that the antigen-presenting ability of DCs is impaired in *Clec1a*$^{-/-}$ mice, explaining why the development of EAE was suppressed in *Clec1a*$^{-/-}$ mice after MOG immunization. In this context, we found that IL-6 and IL-1β pro-

duction, which are thought to be produced mostly in myeloid cells, were impaired in *Clec1a*$^{-/-}$ mice at day 10 after immunization, indicating some abnormalities in these cells, in which low levels of *Clec1a* is expressed. Because these cytokines as well as antigen presentation by DC is important for the induction of Th17 cell differentiation, decreased *Il17a* expression in *Clec1a*$^{-/-}$ mouse dLNs is considered to be caused by a deficiency of *Clec1a*$^{-/-}$ DCs. Consistent with our observations, recently it was reported that *A. fumigatus*-induced pulmonary allergic inflammation is suppressed in *Clec1a*$^{-/-}$ mice associated with a decrease of Th17 cell population, suggesting involvement of Clec1A in the differentiation of Th17 cells [59].

Although it is known that 1,8-dihydroxynaphthalene-melanin in *A. fumigatus* is a ligand for Clec1A, it seems unlikely that this molecule is present in uninfected mice. Thus, our observation suggests presence of an endogenous ligand (s). In this context, it was reported recently that histidine-rich glycoprotein (HRG), which is a multifunctional plasma protein and stimulates human neutrophil phagocytosis and prolongs neutrophil survival, is a ligand for Clec1A [60]. Interestingly, HRG suppresses high mobility group box-1-protein-induced inflammatory responses of endothelial cells through interaction with Clec1A [61].

In summary, we have first shown that Clec1A is involved in the development of EAE by enhancing antigen-presenting activity of DCs. Because Clec1A is highly expressed in blood vessel endothelial cells, it is tempting to speculate that this molecule is also involved in the pathogenesis of EAE by regulating Th17 cell transport through the blood-brain barrier [11]. Clearly, further investigation is necessary to elucidate the mechanism why the development of EAE is suppressed in *Clec1a*$^{-/-}$ mice.

Acknowledgments

This work was supported by Grants-in-Aid from the Ministry of Education, Culture, Sports, Science, and Technology of Japan (18H02671, 20H04954, 21H02394) (Y.I.). Part of this study was carried out in collaboration with Boehringer Ingelheim International GmbH (Y.I.). Y.M. was supported by the Otsuka Toshimi Scholarship Foundation, Japan.

Reference

1. Filippi M, Bar-Or A, Piehl F, Preziosa P, Solari A, Vukusic S, et al. Multiple sclerosis. Nat Rev Dis Primers. 2018; 4: 43. [Medline] [CrossRef]
2. Reich DS, Lucchinetti CF, Calabresi PA. Multiple Sclerosis. N Engl J Med. 2018; 378: 169–180. [Medline] [CrossRef]
3. Bennett J, Basivireddy J, Kollar A, Biron KE, Reickmann P, Jefferies WA, et al. Blood-brain barrier disruption and enhanced vascular permeability in the multiple sclerosis model EAE. J Neuroimmunol. 2010; 229: 180–191. [Medline] [CrossRef]
4. Constantinescu CS, Farooqi N, O'Brien K, Gran B. Experimental autoimmune encephalomyelitis (EAE) as a model for multiple sclerosis (MS). Br J Pharmacol. 2011; 164: 1079–1106. [Medline] [CrossRef]
5. Fletcher JM, Lalor SJ, Sweeney CM, Tubridy N, Mills KH. T cells in multiple sclerosis and experimental autoimmune encephalomyelitis. Clin Exp Immunol. 2010; 162: 1–11. [Medline] [CrossRef]
6. Stromnes IM, Goverman JM. Active induction of experimental allergic encephalomyelitis. Nat Protoc. 2006; 1: 1810–1819. [Medline] [CrossRef]
7. McGinley AM, Sutton CE, Edwards SC, Leane CM, DeCourcey J, Teijeiro A, et al. Interleukin-17A Serves a Priming Role in Autoimmunity by Recruiting IL-1β-Producing Myeloid Cells that Promote Pathogenic T Cells. Immunity. 2020; 52: 342–356.e6. [Medline] [CrossRef]
8. Sutton CE, Lalor SJ, Sweeney CM, Brereton CF, Lavelle EC, Mills KH. Interleukin-1 and IL-23 induce innate IL-17 production from gammadelta T cells, amplifying Th17 responses and autoimmunity. Immunity. 2009; 31: 331–341. [Medline] [CrossRef]
9. Domingues HS, Mues M, Lassmann H, Wekerle H, Krishnamoorthy G. Functional and pathogenic differences of Th1 and Th17 cells in experimental autoimmune encephalomyelitis. PLoS One. 2010; 5: e15531. [Medline] [CrossRef]
10. Lovett-Racke AE, Yang Y, Racke MK. Th1 versus Th17: are T cell cytokines relevant in multiple sclerosis? Biochim Biophys Acta. 2011; 1812: 246–251. [Medline] [CrossRef]
11. Arima Y, Harada M, Kamimura D, Park JH, Kawano F, Yull FE, et al. Regional neural activation defines a gateway for autoreactive T cells to cross the blood-brain barrier. Cell. 2012; 148: 447–457. [Medline] [CrossRef]
12. Glatigny S, Bettelli E. Experimental Autoimmune Encephalomyelitis (EAE) as Animal Models of Multiple Sclerosis (MS). Cold Spring Harb Perspect Med. 2018; 8: a028977. [Medline] [CrossRef]
13. Robinson MJ, Sancho D, Slack EC, LeibundGut-Landmann S, Reis e Sousa C. Myeloid C-type lectins in innate immunity. Nat Immunol. 2006; 7: 1258–1265. [Medline] [CrossRef]
14. Brown GD, Willment JA, Whitehead L. C-type lectins in immunity and homeostasis. Nat Rev Immunol. 2018; 18: 374–389. [Medline] [CrossRef]
15. Drickamer K, Taylor ME. Recent insights into structures and functions of C-type lectins in the immune system. Curr Opin Struct Biol. 2015; 34: 26–34. [Medline] [CrossRef]
16. Tang C, Makusheva Y, Sun H, Han W, Iwakura Y. Myeloid C-type lectin receptors in skin/mucoepithelial diseases and tumors. J Leukoc Biol. 2019; 106: 903–917. [Medline] [CrossRef]
17. Cambi A, Koopman M, Figdor CG. How C-type lectins detect pathogens. Cell Microbiol. 2005; 7: 481–488. [Medline] [CrossRef]
18. Herre J, Willment JA, Gordon S, Brown GD. The role of Dectin-1 in antifungal immunity. Crit Rev Immunol. 2004; 24: 193–203. [Medline] [CrossRef]
19. Ishikawa T, Itoh F, Yoshida S, Saijo S, Matsuzawa T, Gonoi T, et al. Identification of distinct ligands for the C-type lectin receptors Mincle and Dectin-2 in the pathogenic fungus Malassezia. Cell Host Microbe. 2013; 13: 477–488. [Medline] [CrossRef]
20. Koppel EA, Saeland E, de Cooker DJ, van Kooyk Y, Geijtenbeek TB. DC-SIGN specifically recognizes Streptococcus pneumoniae serotypes 3 and 14. Immunobiology. 2005; 210: 203–210. [Medline] [CrossRef]

21. Desamero MJM, Chung SH, Kakuta S. Insights on the Functional Role of Beta-Glucans in Fungal Immunity Using Receptor-Deficient Mouse Models. Int J Mol Sci. 2021; 22: 4778. [Medline] [CrossRef]
22. Sancho D, Joffre OP, Keller AM, Rogers NC, Martínez D, Hernanz-Falcón P, et al. Identification of a dendritic cell receptor that couples sensing of necrosis to immunity. Nature. 2009; 458: 899–903. [Medline] [CrossRef]
23. Yamasaki S, Ishikawa E, Sakuma M, Hara H, Ogata K, Saito T. Mincle is an ITAM-coupled activating receptor that senses damaged cells. Nat Immunol. 2008; 9: 1179–1188. [Medline] [CrossRef]
24. Hodge S, Hodge G, Jersmann H, Matthews G, Ahern J, Holmes M, et al. Azithromycin improves macrophage phagocytic function and expression of mannose receptor in chronic obstructive pulmonary disease. Am J Respir Crit Care Med. 2008; 178: 139–148. [Medline] [CrossRef]
25. van Gisbergen KP, Aarnoudse CA, Meijer GA, Geijtenbeek TB, van Kooyk Y. Dendritic cells recognize tumor-specific glycosylation of carcinoembryonic antigen on colorectal cancer cells through dendritic cell-specific intercellular adhesion molecule-3-grabbing nonintegrin. Cancer Res. 2005; 65: 5935–5944. [Medline] [CrossRef]
26. Singh SK, Streng-Ouwehand I, Litjens M, Weelij DR, García-Vallejo JJ, van Vliet SJ, et al. Characterization of murine MGL1 and MGL2 C-type lectins: distinct glycan specificities and tumor binding properties. Mol Immunol. 2009; 46: 1240–1249. [Medline] [CrossRef]
27. Tang C, Kamiya T, Liu Y, Kadoki M, Kakuta S, Oshima K, et al. Inhibition of Dectin-1 Signaling Ameliorates Colitis by Inducing Lactobacillus-Mediated Regulatory T Cell Expansion in the Intestine. Cell Host Microbe. 2015; 18: 183–197. [Medline] [CrossRef]
28. Saba K, Denda-Nagai K, Irimura T. A C-type lectin MGL1/CD301a plays an anti-inflammatory role in murine experimental colitis. Am J Pathol. 2009; 174: 144–152. [Medline] [CrossRef]
29. Fujikado N, Saijo S, Yonezawa T, Shimamori K, Ishii A, Sugai S, et al. Dcir deficiency causes development of autoimmune diseases in mice due to excess expansion of dendritic cells. Nat Med. 2008; 14: 176–180. [Medline] [CrossRef]
30. Redelinghuys P, Whitehead L, Augello A, Drummond RA, Levesque JM, Vautier S, et al. MICL controls inflammation in rheumatoid arthritis. Ann Rheum Dis. 2016; 75: 1386–1391. [Medline] [CrossRef]
31. Sagar D, Singh NP, Ginwala R, Huang X, Philip R, Nagarkatti M, et al. Antibody blockade of CLEC12A delays EAE onset and attenuates disease severity by impairing myeloid cell CNS infiltration and restoring positive immunity. Sci Rep. 2017; 7: 2707. [Medline] [CrossRef]
32. Seno A, Maruhashi T, Kaifu T, Yabe R, Fujikado N, Ma G, et al. Exacerbation of experimental autoimmune encephalomyelitis in mice deficient for DCIR, an inhibitory C-type lectin receptor. Exp Anim. 2015; 64: 109–119. [Medline] [CrossRef]
33. Colonna M, Samaridis J, Angman L. Molecular characterization of two novel C-type lectin-like receptors, one of which is selectively expressed in human dendritic cells. Eur J Immunol. 2000; 30: 697–704. [Medline] [CrossRef]
34. Sobanov Y, Bernreiter A, Derdak S, Mechtcheriakova D, Schweighofer B, Düchler M, et al. A novel cluster of lectin-like receptor genes expressed in monocytic, dendritic and endothelial cells maps close to the NK receptor genes in the human NK gene complex. Eur J Immunol. 2001; 31: 3493–3503. [Medline] [CrossRef]
35. Thebault P, Lhermite N, Tilly G, Le Texier L, Quillard T, Heslan M, et al. The C-type lectin-like receptor CLEC-1, expressed by myeloid cells and endothelial cells, is up-regulated by immunoregulatory mediators and moderates T cell activation. J Immunol. 2009; 183: 3099–3108. [Medline] [CrossRef]
36. Stappers MHT, Clark AE, Aimanianda V, Bidula S, Reid DM, Asamaphan P, et al. Recognition of DHN-melanin by a C-type lectin receptor is required for immunity to Aspergillus. Nature. 2018; 555: 382–386. [Medline] [CrossRef]
37. Lopez Robles MD, Pallier A, Huchet V, Le Texier L, Remy S, Braudeau C, et al. Cell-surface C-type lectin-like receptor CLEC-1 dampens dendritic cell activation and downstream Th17 responses. Blood Adv. 2017; 1: 557–568. [Medline] [CrossRef]
38. Seifert L, Werba G, Tiwari S, Giao Ly NN, Alothman S, Alqunaibit D, et al. The necrosome promotes pancreatic oncogenesis via CXCL1 and Mincle-induced immune suppression. Nature. 2016; 532: 245–249. [Medline] [CrossRef]
39. Saijo S, Fujikado N, Furuta T, Chung SH, Kotaki H, Seki K, et al. Dectin-1 is required for host defense against Pneumocystis carinii but not against Candida albicans. Nat Immunol. 2007; 8: 39–46. [Medline] [CrossRef]
40. Daley D, Mani VR, Mohan N, Akkad N, Ochi A, Heindel DW, et al. Dectin 1 activation on macrophages by galectin 9 promotes pancreatic carcinoma and peritumoral immune tolerance. Nat Med. 2017; 23: 556–567. [Medline] [CrossRef]
41. Ito T, Hirose K, Norimoto A, Tamachi T, Yokota M, Saku A, et al. Dectin-1 Plays an Important Role in House Dust Mite-Induced Allergic Airway Inflammation through the Activation of CD11b+ Dendritic Cells. J Immunol. 2017; 198: 61–70. [Medline] [CrossRef]
42. Miyabe C, Miyabe Y, Bricio-Moreno L, Lian J, Rahimi RA, Miura NN, et al. Dectin-2-induced CCL2 production in tissue-resident macrophages ignites cardiac arteritis. J Clin Invest. 2019; 129: 3610–3624. [Medline] [CrossRef]
43. Kaifu T, Yabe R, Maruhashi T, Chung SH, Tateno H, Fujikado N, et al. DCIR and its ligand asialo-biantennary N-glycan regulate DC function and osteoclastogenesis. J Exp Med. 2021; 218: e20210435. [Medline] [CrossRef]
44. Olsson T, Zhi WW, Höjeberg B, Kostulas V, Jiang YP, Anderson G, et al. Autoreactive T lymphocytes in multiple sclerosis determined by antigen-induced secretion of interferon-gamma. J Clin Invest. 1990; 86: 981–985. [Medline] [CrossRef]
45. Merad M, Sathe P, Helft J, Miller J, Mortha A. The dendritic cell lineage: ontogeny and function of dendritic cells and their subsets in the steady state and the inflamed setting. Annu Rev Immunol. 2013; 31: 563–604. [Medline] [CrossRef]
46. Ulland TK, Jain N, Hornick EE, Elliott EI, Clay GM, Sadler JJ, et al. Nlrp12 mutation causes C57BL/6J strain-specific defect in neutrophil recruitment. Nat Commun. 2016; 7: 13180. [Medline] [CrossRef]
47. Mekada K, Yoshiki A. Substrains matter in phenotyping of C57BL/6 mice. Exp Anim. 2021; 70: 145–160. [Medline] [CrossRef]
48. Komiyama Y, Nakae S, Matsuki T, Nambu A, Ishigame H, Kakuta S, et al. IL-17 plays an important role in the development of experimental autoimmune encephalomyelitis. J Immunol. 2006; 177: 566–573. [Medline] [CrossRef]
49. Jäger A, Dardalhon V, Sobel RA, Bettelli E, Kuchroo VK. Th1, Th17, and Th9 effector cells induce experimental autoimmune encephalomyelitis with different pathological phenotypes. J Immunol. 2009; 183: 7169–7177. [Medline] [CrossRef]
50. Iwakura Y, Ishigame H, Saijo S, Nakae S. Functional specialization of interleukin-17 family members. Immunity. 2011; 34: 149–162. [Medline] [CrossRef]
51. Zhou L, Ivanov II, Spolski R, Min R, Shenderov K, Egawa T, et al. IL-6 programs T(H)-17 cell differentiation by promoting sequential engagement of the IL-21 and IL-23 pathways. Nat Immunol. 2007; 8: 967–974. [Medline] [CrossRef]
52. Manel N, Unutmaz D, Littman DR. The differentiation of human T(H)-17 cells requires transforming growth factor-beta and induction of the nuclear receptor RORgammat. Nat Immunol. 2008; 9: 641–649. [Medline] [CrossRef]

53. Akitsu A, Ishigame H, Kakuta S, Chung SH, Ikeda S, Shimizu K, et al. IL-1 receptor antagonist-deficient mice develop autoimmune arthritis due to intrinsic activation of IL-17-producing CCR2(+)Vγ6(+)γδ T cells. Nat Commun. 2015; 6: 7464. [Medline] [CrossRef]
54. Werninghaus K, Babiak A, Gross O, Hölscher C, Dietrich H, Agger EM, et al. Adjuvanticity of a synthetic cord factor analogue for subunit Mycobacterium tuberculosis vaccination requires FcRgamma-Syk-Card9-dependent innate immune activation. J Exp Med. 2009; 206: 89–97. [Medline] [CrossRef]
55. Dumas A, Amiable N, de Rivero Vaccari JP, Chae JJ, Keane RW, Lacroix S, et al. The inflammasome pyrin contributes to pertussis toxin-induced IL-1β synthesis, neutrophil intravascular crawling and autoimmune encephalomyelitis. PLoS Pathog. 2014; 10: e1004150. [Medline] [CrossRef]
56. Ronchi F, Basso C, Preite S, Reboldi A, Baumjohann D, Perlini L, et al. Experimental priming of encephalitogenic Th1/Th17 cells requires pertussis toxin-driven IL-1β production by myeloid cells. Nat Commun. 2016; 7: 11541. [Medline] [CrossRef]
57. Reyes TM, Fabry Z, Coe CL. Brain endothelial cell production of a neuroprotective cytokine, interleukin-6, in response to noxious stimuli. Brain Res. 1999; 851: 215–220. [Medline] [CrossRef]
58. Chui R, Dorovini-Zis K. Regulation of CCL2 and CCL3 expression in human brain endothelial cells by cytokines and lipopolysaccharide. J Neuroinflammation. 2010; 7: 1. [Medline] [CrossRef]
59. Tone K, Stappers MHT, Hatinguais R, Dambuza IM, Salazar F, Wallace C, et al. MelLec Exacerbates the Pathogenesis of *Aspergillus fumigatus*-Induced Allergic Inflammation in Mice. Front Immunol. 2021; 12: 675702. [Medline] [CrossRef]
60. Takahashi Y, Wake H, Sakaguchi M, Yoshii Y, Teshigawara K, Wang D, et al. Histidine-Rich Glycoprotein Stimulates Human Neutrophil Phagocytosis and Prolongs Survival through CLEC1A. J Immunol. 2021; 206: 737–750. [Medline] [CrossRef]
61. Gao S, Wake H, Sakaguchi M, Wang D, Takahashi Y, Teshigawara K, et al. Histidine-Rich Glycoprotein Inhibits High-Mobility Group Box-1-Mediated Pathways in Vascular Endothelial Cells through CLEC-1A. iScience. 2020; 23: 101180. [Medline] [CrossRef]